Emerging Multi-Port Electrical Machines and Systems: Past Developments, Current Challenges and Future Prospects

***Abstract*—Distinct from the conventional machines with only one electrical and one mechanical port, electrical machines featuring multiple electrical/mechanical ports (the so-called multi-port electrical machines) provide a compact, flexible, and highly-efficient manner to convert and/or transfer energies among different ports. This paper attempts to make a comprehensive overview of existing multi-port topologies, from fundamental characteristics to advanced modeling, analysis, and control, with particular emphasis on the extensively investigated brushless doubly-fed machines for highly-reliable wind turbines and power split devices for hybrid electric vehicles. A qualitative review approach is mainly adopted but strong efforts are also made to quantitatively highlight the electromagnetic and control performance. Research challenges are identified and future trends are discussed.**

***Index Terms*—Ac machines, doubly-fed, dual-rotor, dual-stator-winding, electromechanical systems, ports, review.**

I. Introduction

ELECTRICAL MACHINES have been widely accepted as the physical devices to accomplish continuous electromechanical energy conversion. In this respect, an electrical machine is described as a coupled field with at least one electrical port characterized by its terminal voltage and current, and one mechanical port characterized by its torque and angular speed (for rotary machine) or force and moving speed (for linear machine) [1]. An electrical port is defined as a set of windings that allows the bidirectional flow of electrical power. Similarly, a mechanical port is defined as a degree of freedom (DOF) of motion that allows the bidirectional flow of mechanical power. For rotating machines, the mechanical shaft is the mechanical port.

Fig. 1 shows the multi-input and multi-output model of electrical machines. Most traditional electrical machines pertain to the single-input single-output configuration which only compasses one electrical port and one mechanical port (m=1, n=1), such as the ordinary direct current machine (DCM), three-phase synchronous machine (SM) with permanent magnet (PM) or wound field excitation, three-phase squirrel-cage induction machine (IM), three-phase variable reluctance machine (VRM), etc. However, other types with more than one electrical port (m>1) or mechanical port (n>1) do exist, such as dual-mechanical-port (DMP) electric machines [2], the slip-ring doubly-fed induction machine (DFIM) [3], dual-stator-winding IMs [4], and brushless doubly-fed induction machines (BDFIMs) [5], to name just a few.

Generally speaking, the number of electrical ports and mechanical ports is arbitrary and only depends on the specific application. The additional electrical ports can be used to increase the power rating, enhance the fault tolerant capability or control the motion/power flow. The mechanical ports are commonly used to decouple the motion/speeds/torques.

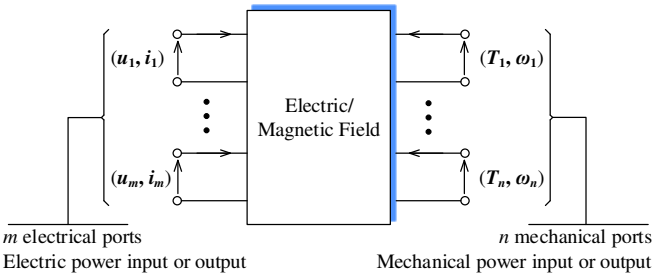

Fig. 1 Multi-input multi-output model of electrical machines.

With the steady improvement of level of electrification globally, multi-port electrical machines have experienced rapid developments in terms of available topologies, analysis and design techniques, and control strategies to meet the increasing needs of power conversion, transfer, hybrid, split, recovery and/or multiple forms of motion at the same time in a wide range of applications during the past decades, as summarized below (including but not limited to):

- Machine tools;
- Robotics;
- Electric vehicles (EVs) and hybrid EVs (HEVs);
- Electric ship propulsion;
- More electric aircraft;
- High power industrial drive;
- Rail transportation;
- Highly-reliable wind power systems;
- Dc/ac/hybrid dc and ac micro-grids.

A. Historical Review of Multi-Port Machines

As early as late 1920s, Alger et al. introduced the dual-winding structure, i.e., the dual electrical port (DEP) feature, to increase the total power capability of large synchronous generators [6]. Franklin used this construction to obtain simultaneous ac and dc outputs in 1973 [7]. This DEP concept was later incorporated into IMs to improve the torque waveform of six-step inverter fed drive (1974) [8], the fault tolerant capability (1994) [9] and the torque density (2002) [10].

Researchers in 1950s paid much effort to the performance and stability analysis of slip-ring DFIM with double supply attempting to achieve speeds higher than the synchronous one determined by the supply frequency [11]. The urgent need for variable speed operation of IMs (stepped or stepless) sparked the idea of cascading two DFIMs, based upon which Smith discovered the doubly-fed synchronous operation of brushless doubly-fed machines (BDFMs) in 1967 [12]. To save space and simplify the winding fabrication process of the cascading

construction, Broad and Burbridge invented what has been later called BDFIM and brushless doubly-fed reluctance machine (BDFRM) in the early 1970s [13], [14].

Multi-DOF machines which have multiple DOFs of motion and are more often termed as actuators, like planar machines, linear-rotary machines and spherical machines mainly sprung up in 1980s to directly realize the complex motion without any mechanical transmission.

Electrical machines and systems with practical DMP feature mainly appeared after 2000 driven by the rapid development of EV/HEV drivetrains. Specifically, in 2002, Eriksson and Sadarangani presented a split-power hybrid system by combining two concentrically-arranged PM machines (termed as four quadrant transducer (4QT)) to decouple the speeds and torques of two mechanical ports [15]. Hoeijmakers implemented a similar system with an IM-based DMP machine and named it as the electric variable transmission (EVT) in 2004 [16]. Xu systematically analyzed the basic structures and operational principles of this multi-port machine family with two electrical ports and two mechanical ports and developed the concept of DMP machine [2]. Since then, research scientists and engineers from all over the world have conducted extensive research on various multi-port topologies.

B. Scope and Classification

To date, quite a number of electrical machine topologies have been reported to fall into the category of multi-port machines, and various terminologies, such as doubly-fed, doubly-excited, dual-stator-winding, dual-rotor, etc., have been used to characterize and discriminate them from the single-electrical-port (SEP)+single-mechanical-port (SMP) machines.

This paper makes an extensive overview of the multi-port electrical machines featuring multiple rotors and/or multiple windings, mainly including the DEP+SMP machines (slip-ring DFIMs and various brushless versions, the dual-stator-winding machines), the SEP+DMP machines (the PMIM, the machine integrated PM gear (PMG), and the magnetically-geared dual-rotor machine (DRM)), the DEP+DMP machines (various conventional and newly-emerged EVTs), the multiple-electrical-port (MEP) machines (e.g., multiphase machines with multiple three-phase or five-phase winding sets) and multi-DOF machines. Extended configurations, like the multi-machine systems are also considered. Machines with electrical excitation and hybrid excitation are excluded from the scope of this overview because the dc-excitation coils are not effective electrical ports. The detailed classification of electrical machines by numbers of electrical and mechanical port is shown in Fig. 2.

This paper is organized as follows. Section II, III, IV deal with the DEP+SMP, SEP+DMP, and DEP+DMP machines respectively. MEP machines and multi-DOF machines are discussed in Section V and Section VI, followed by the multi-machine systems in Section VII. Section VIII concludes the paper and predicts future development trends.

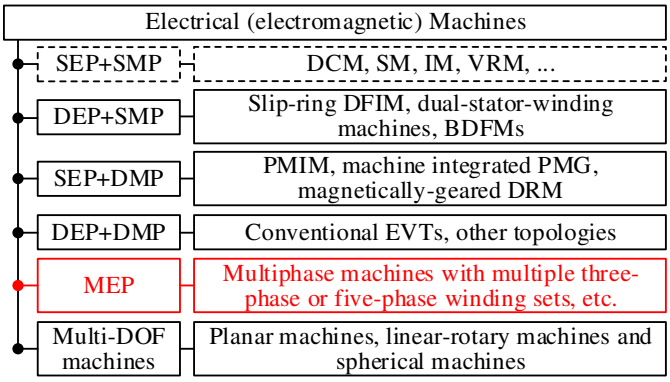

Fig. 2 Classification of electrical machines.

II. DEP+SMP Machines

DEP+SMP machines have two sets of physical winding involved in the electromechanical energy conversion, whose numbers of phases and pole pairs can be the same or different. The electrical angular frequencies of the two winding sets are denoted by ω_1 and ω_2 respectively. Moreover, it is assumed that $\omega_1(\omega_2)$ is positive if the rotating direction of the magnetomotive force established by the corresponding winding set is anti-clockwise, otherwise it is negative. The pole pairs are p_1 and p_2. The synchronous speed of rotor in rad/s is denoted as ω_r.

A. Slip-Ring DFIM

The supply frequencies and the rotating speed of the slip-ring DFIM satisfy:

$$\omega_1 - \omega_2 = p_1\omega_r = p_2\omega_r \tag{1}$$

The DEP feature allows the slip-ring DFIM to be configured as singly-fed IM (one of the two electrical ports is short-circuited directly or through resistances), wound-rotor SM (one of the two electrical ports is connected to a dc source, i.e., ω_1=0 or ω_2=0) or DFIM (both electrical ports are supplied by ac sources, i.e., $\omega_1\neq0$ and $\omega_2\neq0$), adding flexibility in the drive system design.

When operated as a DFIM, it can further be configured in SEP or DEP control mode. Fig. 3 shows the SEP control configuration which enables the bidirectional flow of slip power while keeping the frequency of one electrical port constant regardless of the speed variation; so it is quite suitable for limited-speed range applications where variable speed constant frequency is required and the rating of power converter needs to be minimized, such as wind power generation [3] and flywheel energy storage [17].

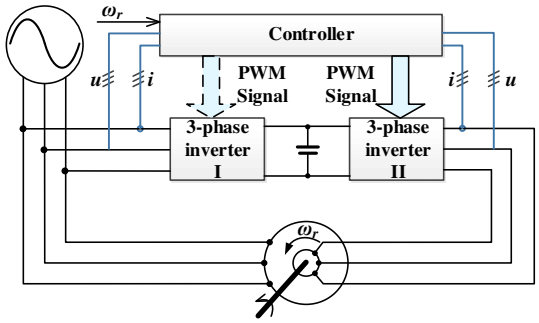

Fig. 3 SEP control configuration of DFIM.

To achieve the full-speed-range operation of a SEP control configuration, the power converter has to be rated fully so the benefit of low cost due to partially-rated power electronics is lost. Alternatively, the power connection to the stator can be switched on the fly between a constant dc and constant voltage constant frequency ac supply, which yields the so-called switched DFIM, as depicted in Fig. 4. A typical switched DFIM drive can continuously operate over a speed range of ±1.5 p.u. (normalized relative to the ac source synchronous speed) with a rotor converter rated only 1/3 of the maximum shaft power [18]. In addition, the switched DFIM drive can offer seamless interface to the ac grid with controllable power factor and reactive power support [19]. The bumpless switching can be realized by low-cost silicon controlled rectifiers (SCRs) [20].

The switched DFIM drive has two modes of operation: low-speed mode and high-speed mode. In low-speed mode, the stator of the slip-ring DFIM can be either short-circuited to form an inverted singly-fed IM [21] or connected to a dc supply and the machine is equivalent to an inverted wound-rotor SM [22]. In high-speed mode, the stator of the switched DFIM is connected to the ac supply and the rotor winding is driven by a back-to-back converter. The switched DFIM can be controlled to achieve smooth operations in and through the two modes. A holistic comparison between these two low-speed configurations was conducted showing that the sharing of the magnetizing current between the stator and the rotor, tolerance on the structural noise and vibration have a significant influence on the choice of the preferable switched DFIM topology [23].

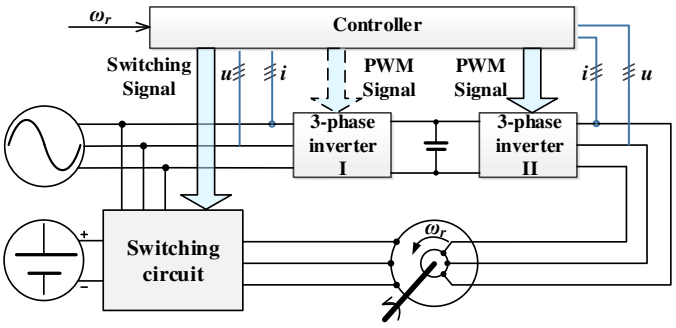

Fig. 4 The switched DFIM drive.

On the contrary, the DEP control configuration, as illustrated in Fig. 5, changes inputs of both electrical ports simultaneously to achieve extended speed range with rated torque capability for full-speed-range applications [24], [25].

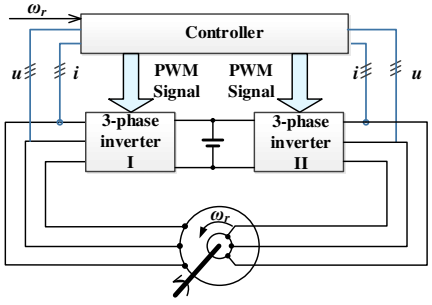

Fig. 5 DEP control configuration of DFIM.

The rotor voltage requirements, which also reflect the volt-ampere rating of the power electronics versus speed ranges of different DFIM configurations are summarized in Fig. 6.

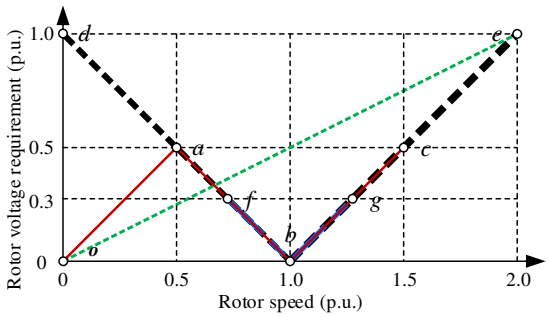

Fig. 6 The rotor voltage requirements of different DFIM configurations. *fbg*: SEP control of DFIM for limited-speed-range application; *dbe*: SEP control of DFIM for full-speed-range application; *oabc*: switched DFIM; *oe*: DEP control of DFIM.

B. Dual-Stator-Winding Machines

The dual-stator-winding machines hereto refer to squirrel-cage induction/synchronous (PM or wound-field)/variable reluctance machines equipped with an extra stator winding set. The airgap field modulation phenomenon in dual-stator-winding machines discussed in this section is synchronous [26], that is, the short-circuited coils, simple salient reluctance blocks or multiple flux barriers make no change to the principal pole pair number of magnetizing magnetomotive force. Different from the classification in [4], the BDFIM with a nested-loop rotor is excluded from the dual-stator-winding IM considering the difference in working principle rather than the similarities in physical construction. All dual-stator-winding machines make it possible to extend the power range of the drives beyond the power capability of a single inverter. Additionally, the inherent redundancy provides better reliability.

The steady-state relationship between supply frequencies and mechanical rotating speed under synchronous operation can be summarized as

$$\omega_1/p_1 = \omega_2/p_2 = \omega_r \tag{2}$$

For the dual-stator-winding IMs, the pole pairs of the two stator windings can be the same or not because the die-cast squirrel-cage rotor is a passive device and its pole pair completely depends on the stator windings. In contrast, for the dual-stator-winding SMs/VRMs, the pole pairs of the two stator winding sets should be identical.

The two distributed stator windings are wound for the same number of poles in the first design among which machines with two three-phase winding sets may be the most popular configurations. The two three-phase stator winding sets can be electrically displaced from each other by an electrical angle of 0º (usually termed as dual three-phase IM) [27], 30º (asymmetrical six-phase IM) [28-36] or 60º (symmetrical six-phase IM) [27], [37], though theoretically an arbitrary displacement is viable [8]. The neutral points of the two three-phase winding sets can be either connected together or isolated, showing differences in control of zero sequence current (e.g., zero sequence current can be made full use of to

enhance the torque production under healthy [10] or faulty conditions [33]) and dc-bus utilization [38]. IMs with dual stator-winding sets, especially the asymmetrical six-phase IMs, are conventionally used for variable speed drive where fault-tolerant operation is required or volt-ampere rating per three-phase winding set is constrained. Recent explorations of using dual three-phase-winding IMs in wind energy conversion system with fully-rated power converter [31], integrated onboard battery chargers for EVs [39], dc [40], ac [41], or hybrid dc and ac [32] micro-grids show the promising prospect of such machines in electric energy conversion and transfer.

In the other design, the two stator windings are wound for different pole numbers with no displacement between them. Appropriate pole pair combination (3:1) and operation mode (synchronous operation) allow a significant torque density improvement of this dual-stator-winding IM design [42]. When used as a generator, it can generate two different voltage levels, which can be further used to boost the current capacity (outputs in parallel connection) and voltage level (outputs in series connection) [43].

Compared with the dual-stator-winding IMs, the dual-stator-winding PMSMs are marginally dealt with. Research on the dual-stator-winding PMSMs focuses on the enhancement of fault-tolerant capability by means of improved design, for instant, using the fractional-slot concentrated windings [44], or fault-tolerant control strategies [45], [46]. The measured dynamic performance under one-phase (phase D) open-circuit fault for a T-type neutral point clamping (T-NPC) dual-stator-winding PMSM drive is shown in Fig. 7. The periodic torque ripple of faulty winding Te2 can be well compensated by the healthy winding torque Te1, and the electromagnetic torque in post-fault operation can accurately track its reference value.

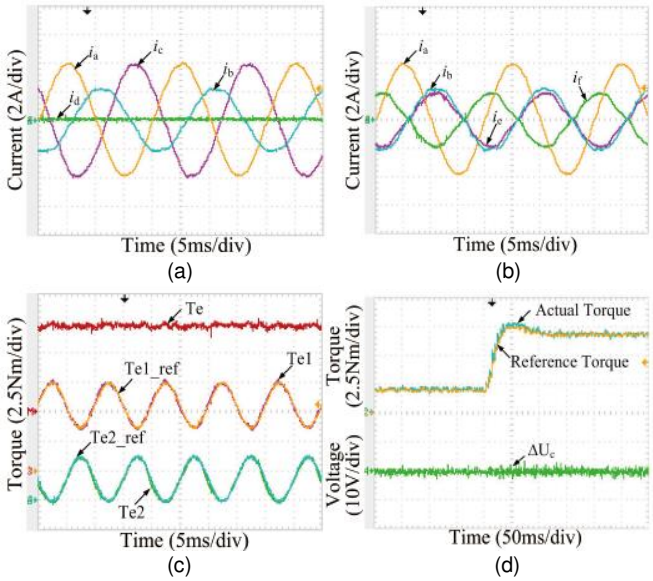

Fig. 7 Measured drive performance under one-phase (phase D) open-circuit fault with fault tolerant control: (a) Currents of phase A, B, C and D; (b) Currents of phase A, B, E and F; (c) Torque; (d) Transient performance [46].

The dual-stator-winding feature has also been applied to other machine topologies to bring about new DEP+SEP machines with fault-tolerant capability and high reliability, such as the synchronous reluctance machine [47] and switched reluctance machine [48].

C.BDFM

BDFMs, the brushless versions of the slip-ring DFIM, work by two distinct operation principles, that is, cascading and modulation. The cascading types can be achieved by cascading another slip-ring DFIM [12], a rotary transformer [49] or a rotary power converter [50] (at the same time with shafts mechanically coupled) to transfer power between rotating rotor winding and stationary control ports, as shown in Fig. 8.

The modulation type employs the asynchronous modulation behaviors of the specially-designed rotors ($N_r = p_1 \pm p_2$, where p_1 and p_2 are the principal pole pair numbers of stator windings and N_r number of modulation segments) to couple both stator windings indirectly to realize electric power transfer and conversion among two electrical ports and the mechanical port. The available rotor constructions are nested-loop rotor [13], simple-salient-pole rotor [51], axially-laminated-anisotropic rotor and multi-barrier rotor [14], as illustrated in Fig. 9.

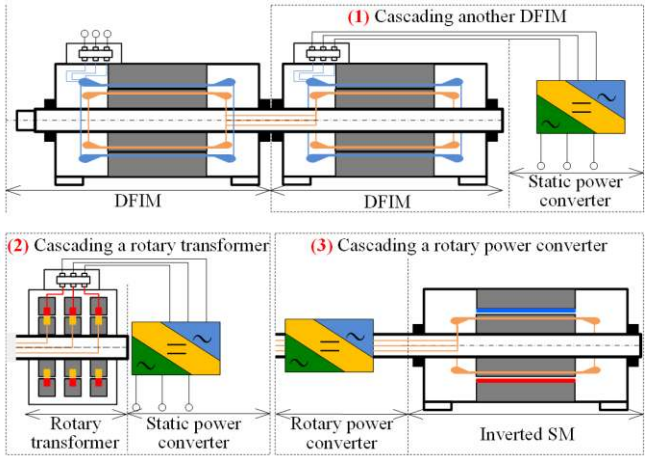

Fig. 8 BDFMs working by the principle of cascading: (1) cascading another DFIM, (2) cascading a rotary transformer, (3) cascading a rotary power converter.

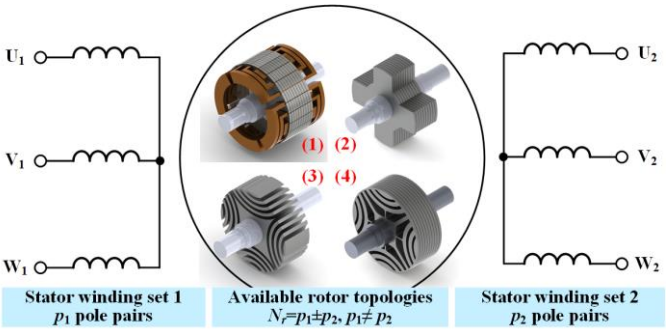

Fig. 9 BDFMs working by the principle of modulation: (1) nested-loop rotor, (2) simple salient-pole rotor, (3) axially-laminated anisotropic rotor, (4) multi-barrier rotor.

Though these topological variations differ from each other significantly in mechanical construction and electromagnetic parameters, they share similar dynamic and steady-state models [52-54], modes of operation and available operating regimes

[55].

Both types comply with the steady-state relationship between supply frequencies and mechanical rotating speed under doubly-fed synchronous operation as given by

$$\omega_1 \pm \omega_2 = p_{eq}\omega_r = (p_1 \pm p_2)\omega_r \tag{3}$$

where $p_{eq}=p_1\pm p_2$ is the equivalent pole pair of BDFM. Plus sign in (3) is used if the two rotor windings of the cascading type are interconnected in reversed phase sequence or the number of modulation segments of the modulation type is made the sum of the pole pairs of two stator windings; otherwise minus is used. The sign between ω_1 and ω_2 is determined by the rotor structure.

The mutual reactance, which reflects the cross-coupling capability of BDFMs, is nearly constant in the full speed range except in the vicinity of the synchronous speed of PW if rotor winding exists. The cross-coupling characteristics of a dual-stator BDFIM in both current and voltage control modes are shown in Fig. 10(a) and (b) respectively [56].

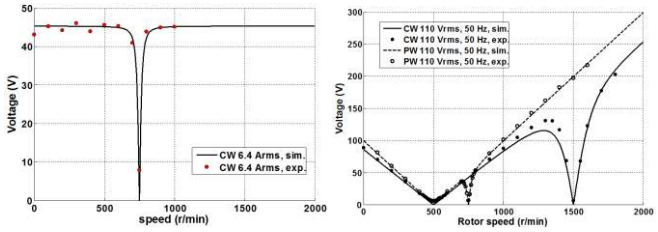

(a) (b)

Fig. 10 Cross-coupling characteristics of DS-BDFIM [56]. (a) Current control mode, (b) Voltage control mode.

With this nearly linear cross-coupling feature, the approximately decoupled active-reactive power control can be realized. The typical stator-flux-oriented control (SFOC) block diagram of BDFMs is shown in Fig. 11(a) [54], [57-59]; the step responses of independent active and reactive power control are shown in Figs. 11(b) and (c) respectively [59].

Substantial knowledge on BDFMs has been generated from the past decade's exhaustive research, which may be summarized as follows:

- Topological analysis of airgap field modulation phenomenon in BDFMs [26], [60], [61];
- Emergence of new or improved machine topologies for higher torque density and/or efficiency [49], [50], [62-64];
- Modeling and performance analysis taking into account the influence of harmonics, saturation and iron loss [65-68];
- Design optimization considering the multi-port and multi-harmonic feature [58], [69-71];
- Dynamic modeling and fundamental control, mainly for the cascading type and BDFIM due to their complex construction [72-80];
- Control strategies and performance evaluation in stand-alone [81-83] and grid-connected wind power scenarios, especially on low-voltage ride-through (LVRT) [84-86], unbalanced or grid-fault conditions [57], [87], [88], etc.
- Exploration in sensorless operation [89-92].

Several large BDFMs have been built and tested as the milestones on the way to multi-megawatt BDFM-based power generation systems (e.g. the Cambridge 250 kW BDFIM [85], [86]). BDFMs are unique carrier for the research of widely-observed airgap field modulation phenomenon and behaviors of asynchronous spatial harmonics which is of great theoretical significance for electrical machinery. Nonetheless, technically, the relatively low torque density and efficiency, poor quality of output voltage and additional vibration (for the modulation type) pose tough challenges on its potential commercialization.

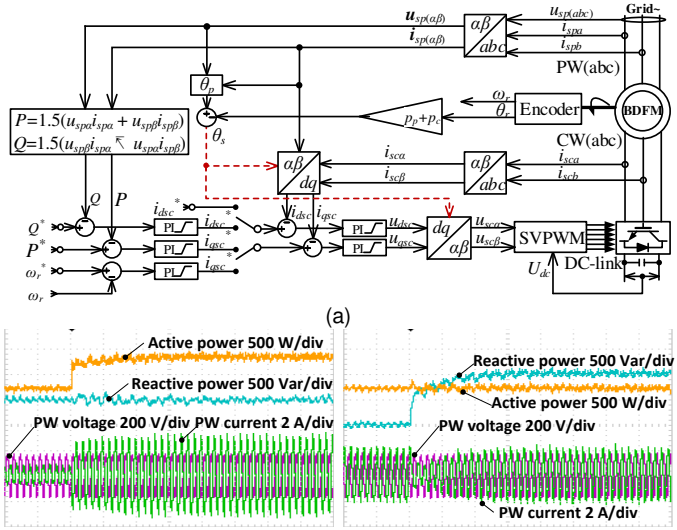

Fig. 11. SFOC of BDFM. (a) Block diagram [54], [57-59], (b) Step change in active power (100 ms/div) [59], (c) Step change in reactive power (100 ms/div) [59].

III. SEP+DMP MACHINES

A. PMIM

The PMIM makes use of an additional free-rotating PM rotor inside the cage rotor, outside the cage rotor or between the stator and the cage rotor of an IM to reduce the magnetizing current and consequently improve the overall power factor and efficiency [93]. Though it has two mechanical ports, the PM rotor is set free and only the cage rotor serves as the active mechanical port. Therefore this SEP+DMP topology is usually used as a SEP+SMP machine, as indicated by

$$\begin{cases} p_{sw}\omega_{sw} = p_{ir}\omega_{ir} = p_{or}\omega_{or} \\ p_{sw} = p_{ir} = p_{or} \end{cases} \tag{4}$$

where ω_{sw}, ω_{ir} and ω_{or} are synchronous speed of stator winding, inner rotor, and outer rotor, respectively. p_{sw}, p_{ir}, and p_{or} are pole pairs of stator winding, inner rotor and outer rotor, respectively.

A typical topology with PM rotor between the stator and the squirrel-cage rotor is depicted in Fig. 12(a). It was once investigated as an alternative solution for direct-drive wind power harvesting [94]. The electrical equivalent circuit, as illustrated in Fig. 12(b), takes into account the core loss as well as the PM excitation and was derived for accurate performance

prediction [95]. It was found that the built-in PM rotor could decrease the magnetizing inductance and the effective turn ratio thus providing a higher power density [96]. Combined with an extra PM rotor, the PMIM essentially works likes an improved squirrel-cage IM so that the speed range as a direct grid-connected generator is still rather limited [97].

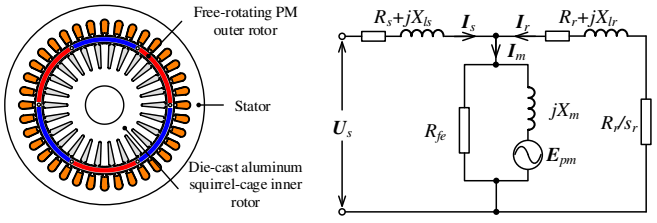

Fig. 12 The PMIM, (a) Topology, (b) Electrical equivalent circuit for steady-state analysis [96].

A dual-rotor radial-flux toroidally wound PM machine was proposed to substantially improve the torque-to-volume ratio and efficiency [98]. The pole pairs and synchronous speeds of the two rotors are identical so they are fixed together to drive a common shaft. A similar vernier type and SRM were presented in [99] and [100] respectively.

B. Machine Integrated PMG

The concept of integrating a PMSM with a coaxial magnetic gear was first described by Venturini in 1993 [101]. Mainly two topologies have been investigated, that is the magnetic-geared outer rotor PM machine [102] (also termed as machine integrated PMG [103]) shown in Fig. 13(a), and the "pseudo" direct-drive machine [104] shown in Fig. 13(b).

Taking the outer stator type as an example, theoretically, it has two mechanical ports (two rotating parts) and an electrical port (the stator winding). The mechanical speeds are constrained by

$$\begin{cases} p_{sw}\omega_{sw} = p_{ir}\omega_{ir} \\ p_{ir}\omega_{ir} + p_{spm}\times 0 = \left(p_{ir} + p_{spm}\right)\omega_{or} \end{cases} \tag{5}$$

where p_{spm} is the pole pairs of PMs mounted on the rotor.

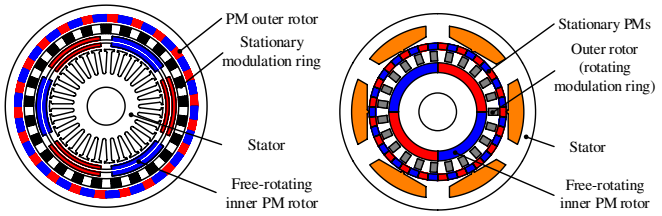

Fig. 13 The machine integrated PMG. (a) Outer rotor type, (b) Outer stator type.

Similar to PMIM, one of the two mechanical ports is usually set free and the whole machine degrades into a SEP+SMP topology.

The machines shown in Fig. 13 are conventionally conceived suitable for low-speed high-torque applications. An attractive torque density (>60 kNm/m^3) at a high power factor (≥0.9) was reported for a naturally air-cooled machine integrated PMG [104]. In addition, they are much easier to reach saturation even with a low armature current, resulting in a lower overload capability and utilization of PM materials. Recent research results show that they also have high potential in EVs as a traction motor by carefully designing the decoupling of the magnetic gear, PMSM and the leakage inductance, improving the mechanical design and reducing the rotational losses [105]. The experimentally verified torque density in terms of active volume reaches 99.7 kNm/m^3 [106]. No commercial applications of the machine integrated PMG have yet emerged probably due to the expectations for better performances, easier manufacture and lower cost.

C. Magnetically-Geared DRM

The magnetically-geared DRM has two active rotating parts (mechanical ports) and a stator winding set (electrical port) located in the stator slots, as shown in Fig. 14(a). Based on the analogy between the magnetically-geared DRM and the mechanical planetary gear, the magnetically-geared DRM can be applied in HEVs to replace the planetary gear and the generator [107]. Under this circumstance, the mechanical power outputted by the internal combustion engine (ICE) will be split into two parts. The first part is directly transferred to the drive axle by the inner rotor and the second part is converted into electric power by the stator winding to supply the motor and charge the battery as well.

The mechanical speeds of the three parts are subjected to the following relationships:

$$\omega_{sw} + \frac{p_{ir}}{p_{sw}}\omega_{ir} = \left(1 + \frac{p_{ir}}{p_{sw}}\right)\omega_{or} \tag{6}$$

where N_{or} is the number of ferromagnetic segments and $N_{or}=p_{sw}+p_{ir}$. T_s, T_{ir} and T_{or} are electromagnetic torques acted on stator, inner rotor and outer rotor respectively. The magnetically-geared DRM can decouple the rotating speeds of the two mechanical ports with torque constraints. The proportional torque relations have been demonstrated by steady-state tests on a prototype, as shown in Fig. 14(b) [108].

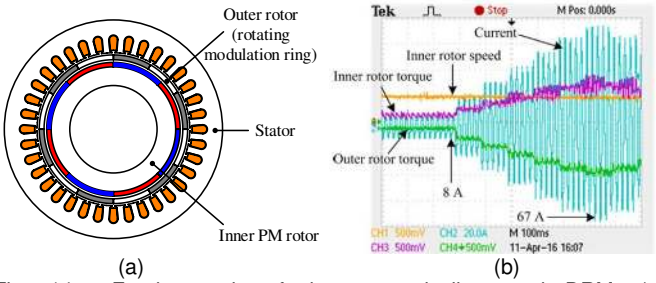

Fig. 14 Fundamentals of the magnetically-geared DRM, (a) Cross-section view, (b) Experimental steady-state torque relations (Torque: 25 Nm/div, Speed: 500 r/min/div, p_{sw} =2, p_{ir} = 4, N_{or} = 6) [108].

The speed/torque control of the magnetically-geared DRM is nearly the same except that the effective magnetic field component produced by the asynchronous modulation behavior of the modulation ring should be oriented according to the measured positions of two rotors [109]. The control block diagram of the vector control of the magnetically-geared DRM is shown in Fig. 15.

An engineering prototype with complementary structure (51 Nm at 2250 r/min, water cooled) was designed, optimized, fabricated and tested together with a 1.0 L naturally aspirated ICE (71 Nm at 3000-3500 r/min, 34.7 kW at 5200 r/min) and a traction motor (200 Nm at 1500 r/min) [109], [110]. The electromechanical energy conversion efficiency tested when ICE is turned off and the magnetically-geared DRM operates in generating mode is shown in Fig. 16(a). It can be seen that the magnetically-geared DRM is definitely not a good energy converter in terms of efficiency. However, as a power split device, the efficiency is attractive especially in the region around direct drive where the speeds of ICE and traction motor are close, as shown in Fig. 16(b). A good choice of the direct drive speed can result in a rather efficient power transmission.

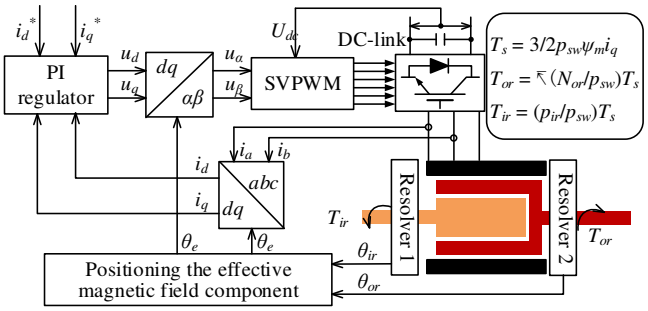

Fig. 15 Vector control of the magnetically-geared DRM [108].

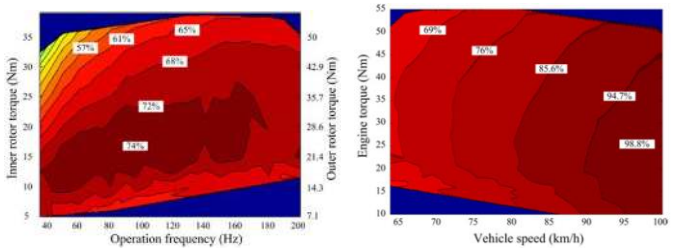

(a) (b)

Fig. 16 Efficiency maps of the magnetically-geared DRM based power split device [108]. (a) Electromechanical energy conversion efficiency (P_{ICE} = 0, the magnetically-geared DRM works as a generator), (b) Power split efficiency (constant engine speed 2800 r/min with varying vehicle speed).

Considering the fact that the modulation efficiency of multi-barrier modulator is generally higher than that of the simple-salient-pole modulator [26], a topology was proposed to improve the torque density and utilization of PM materials [111]. It interchanges the positions of the PM rotor and the modulation ring, and replaces the simple-salient-pole modulator with the multi-barrier one.

IV. DEP+DMP MACHINES

In existing literature, DEP+DMP machines together with the associated power electronics are referred to as "4QT" [15], "EVT" [16] or "DMP machine" [2]. They have been invented to serve as power split devices in HEVs to split the power to the wheels in a part directly coming from the ICE and a part exchanged with the battery. Different from the magnetically-geared DRM, the DEP+DMP machine combines the power split and the two electrical machines into one electromagnetic device.

The DEP+DMP machines consist of a wound stator, a wound inner rotor (with brushes and slip-rings) and an outer rotor, which may have a dual-layer PM array [15], a single-layer PM array [2], a dual-layer squirrel cage [16] or a single-layer squirrel cage [112], as shown in Fig. 17(a)-(d) respectively. For the dual-layer rotor topologies, the thickness of the yoke of the outer rotor has a significant influence on the coupling between the stator and inner rotor windings. In practice, the outer rotor yoke of the dual-layer PM rotor EVT is usually designed thick enough to achieve decoupled control of the outer machine (stator + outer rotor) and the inner machine (outer rotor + inner rotor) [113], which resembles that of the conventional PMSM. While the yoke thickness of the outer dual-layer squirrel-cage rotor is made thin to reduce weight and volume so the inner machine and outer machine are not magnetically separated anymore [16] and the electromagnetic behavior of the EVT differs from two IMs a lot. The coupling also exists in two single-layer rotor topologies, which complicates the modeling and control [114], [115]. Hybrid-excited outer rotor has been recently introduced to change the stator flux while maintaining the inner rotor flux unchanged aiming at reducing iron losses when the stator torque is low [116]. The power split function can also be performed by a switched reluctance DEP+DMP machine [117]. The rotating speeds and supply frequencies in these synchronously modulated EVT are subject to the following relationships:

$$\begin{cases} \omega_1 / p_1 = \omega_{or} \\ \omega_1 + \omega_2 = p_1 \omega_{ir} = p_2 \omega_{ir} \end{cases} \tag{7}$$

As indicated by (7), the electrical frequencies of stator and inner rotor need to be controlled simultaneously to synchronize the different magnetic fields to one unique rotating field.

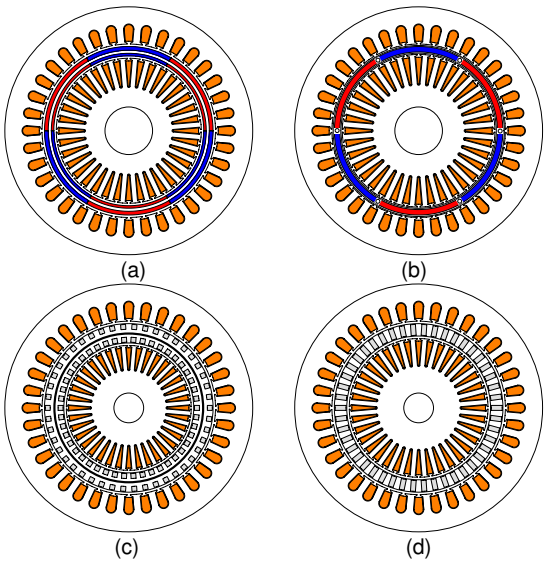

(a) (b) (c) (d)

Fig. 17 Variations of EVT. (a) Dual-layer PM rotor, (b) Single-layer PM rotor, (c) Dual-layer squirrel-cage rotor, (d) Single-layer squirrel-cage rotor.

Multiple operation modes required by practical HEVs have been demonstrated to be available using a single-layer PM rotor EVT in [118]. The corresponding control block diagram is shown in Fig. 18. The concentric arrangement of two rotors and

the high-frequency deep-slot feature [119] of inner rotor poses new challenges on the design of cooling system [120], [121] and mechanical reliability [122], implying that EVTs should be designed in a multiphysics framework [123].

A procedure to define the technical requirements of an EVT was presented in [124]; it was based upon a comparative study between the well-known Prius II and a virtual EVT-based HEV built with the same components and has shown comparable fuel consumptions [125]. The transmission efficiency of the DEP+DMP machine is higher than the magnetically-geared DRM [126]. The rules to choose the direct-drive speed also applies to DEP+DMP machines because the transmission efficiency decreases remarkably as the speed deviates from the direct drive point.

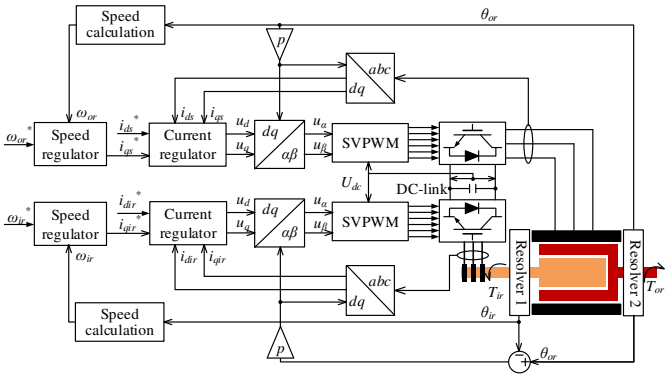

Fig. 18 Block diagram of PM DMP machine system (p=p_1=p_2) [118].

A different arrangement of DEP+DMP machine (fractional horse power) using two asynchronous magnetic fields to drive two independent output shafts for variable-speed air conditioners was proposed in [127]. It makes full use of the thick stator yoke and dissimilar pole pairs to decouple the outer machine from the inner machine, thus being usable as a brushless EVT. A number of EVT topologies working by asynchronous modulation have also been proposed recently [128], [129].

V. MEP Machines

The electrical port number of DEP+SMP and DEP+DMP machines can be further extended to be larger than 2 (i.e., m ≥ 3). The commonest MEP machines are multiphase electrical machines (symmetrical or asymmetrical) with m winding sets and k phases per winding set, where k is a prime number, and (2) still holds true for any two of the winding sets [130]. In addition, each winding set can be star-connected with a single neutral point or m isolated neutral points, polygon-connected or even totally open-end [130-132] in principle. So far, quite a few MEP machines have been put into practical applications, such as the triple three-phase PMSM for an ultrahigh-speed elevator [133], the quadruple three-phase SM for high-power turbo-compressor drive [134], the triple five-phase IM for electric ship propulsion [135] and the PM brushless machines with a multitude of independent modules in parallel [136], [137], etc.

VI. Multi-DOF Machines

Multi-DOF machines, mainly including the planar machine, the linear-rotary machine and the spherical machine, are invented to eliminate the intricate mechanical transmission in combined multiple single-DOF machines based on classical IM, PMSM and VRM. The moving components are usually made to be dual-layer and comprise of a conducting layer and either a back iron for IM, or surface-mounted for PMSM and or a simple-salient-pole for VRM, considering the ease of manufacture. They all feature multiple winding sets for position/orientation/speed/torque control and multiple DOFs of motion, and have the merits of high mechanical integration, high reliability and complete controllability.

A. Planar Machine (2/3-DOF)

Planar motors are described as 2-DOF (the translation coordinates x and y) or 3-DOF (including the rotation coordinate φ_z). Much attention has been paid on the planar PMSMs, which have moving magnets and stationary coils [138], or moving coils and stationary magnets [139]. The moving-magnet planar PMSM needs no cable to the mover and only the coils below and near the periphery of the magnet array can produce force while the moving coil type seems more suitable for long stroke applications since the movers can move freely. 3-DOF planar induction machines (PIMs) were usually achieved by combining at least three linear or curved IM modules [140-142].

B. Linear-Rotary Machine (2-DOF)

The linear-rotary machine has two DOFs (the translation coordinate z and the rotation coordinate φ_z), so it is also termed as the z-φ_z module. It has wide applications in the manufactures of mechanical tools such as robots for chip production lines, robotic arms, injection machines, and boring machines, where linear, rotary or helical motions are required.

Generally, there are three types of z-φ_z modules, that is,

- A linear machine drives a trolley which holds a rotary machine [143];
- The moving parts of the spatially separated linear and rotary machines drive the same shaft [144], [145];
- The linear and rotary machines overlap each other in space. For example, the design in [146] consists of a checkerboard magnet array mover and a common stator equipped with two orthogonal winding sets (one oriented in the circumferential direction and the other axial).

C. Spherical Machine (2/3-DOF)

The spherical machine can be dated back to 1955, when Williams and Laithwaite developed a spherical IM (SIM) to achieve the continuous variable speed operation of utility supplied squirrel-cage IM by adjusting the mechanical angle θ between the moving directions of the rotor and the traveling magnetic field established by a curved inductor [147], as shown in Fig. 19. Following the idea presented in [147], a 2-DOF SIM composed of a two-layer rotor and five curved inductors (four 1-DOF side-inductors and one 2-DOF inductor with crossed windings below the rotor) was developed to achieve unlimited

angular range [148]. By relocating the four curved inductors, a 3-DOF SIM can be achieved. Owing to the angular velocity and orientation sensed by four optical mouse sensors, the closed loop control was realized [149], showing fast dynamic responses in both angular velocity and position control. The corresponding control block diagram is shown in Fig. 20.

Research on other available SIM topologies is also ongoing. A meaningful exploration was the shell-like SIM using zenithal traveling field produced by azimuthal-oriented windings which can significantly ease the assembly by reducing the overlapping of end turns [150].

A spherical PM machine composed of an entire surfaced-mounted PM spherical rotor and stator-mounted coils have been developed to achieve either 2-DOF or 3-DOF motion [151]. A design with variable pole pitch (112 rotor PMs and 96 concentrated stator poles) was implemented to achieve high torque (≥40 Nm) with a good position accuracy [152]; however, the large number of current commands complicates the control system design. The control of the orientation of a continuously rotating shaft was for the first time realized on a special spherical PM VRM in an open-loop fashion [153].

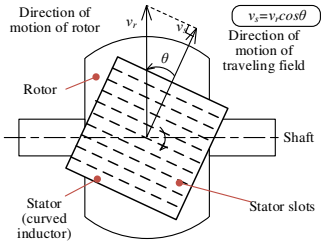

Fig. 19 The spherical induction motor.

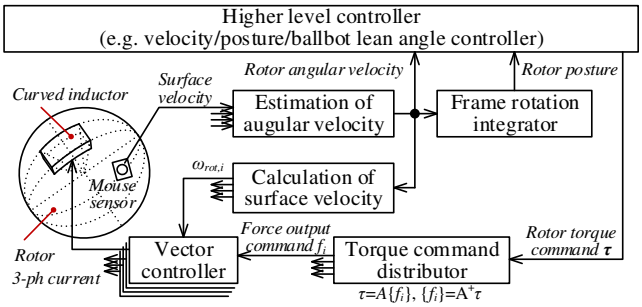

Fig. 20 Control block diagram of the spherical induction machine.

VII. Multi-Machine Systems

Electrical ports of different machines can be connected in series [154], parallel [155], or cascade [156] to form new systems. Similarly, mechanical ports can also be mechanically coupled via torque or speed [157], [158] or completely independent [159]. This flexibility in configuration brings the multi-machine systems with additional benefits over conventional SEP+SMP machines, such as better torque-speed characteristics and efficiency [157], [158], [160], lower system cost [161-164] and enhanced fault-tolerance [165], etc.

VIII. Conclusion and Future Trends

The concept of multi-port electrical machine is introduced to discriminate a whole host of emerging machine topologies from the conventional single-input single-output machines. Benefiting from the multiple input/output ports, the multi-port machines have significant flexibility in drive system design, leading to more application-adapted and effective solutions for various application scenarios. On the one hand, the multi-port feature allows more flexible power flow and more efficient system energy conversion and/or transfer; on the other hand, it poses more challenges on the operation control and mechanical reliability due to highly-integrated design and assembly. The multi-port machines share the same basic working principles as their single-input single-output counterparts, that is, the principles of SM, IM and VRM. They can be developed from the basic single-input single-output topologies by means of cascading or modulation.

The multi-port feature produces more DOFs for controller design and the development of multi-port machines significantly depends on the progress in modern power electronics, advanced control techniques, advanced manufacturing, sensing, etc.

To conclude, both the academic and industrial communities have witnessed the rapid development of the multi-port electrical machines during the past decades. Some have already been put into commercial use on a large scale, some are on the research and development stage, and others are under extensive academic research. For example, the slip-ring DFIM has been a predominant solution for wind turbine and high-power drive. The Tesla dual-motor drive system has become really a milestone for pure EVs. In addition to these successful commercial products, the EVT and BDFMs are nearly on the market. The majority of the rest remains to be developed and more investigations are underway. There is every reason to believe that the multi-port electrical machines and systems will play an irreplaceable role in efficient and intelligent utilization of energy today and in the near future.

Based on the presented survey, the future development trends of multi-port electrical machines may lie in the following aspects:

- Innovative design and multidisciplinary optimization of electromechanical energy conversion systems that can best fit the application scenarios and fully exploit the flexibility introduced by the multi-port feature. For instance, different from established EV traction technologies, the revolutionary "front + rear" dual-motor configuration adopted by the Tesla all-wheel drive P100D Model S employs two IMs with distinctly different torque-speed characteristics and efficiency maps to substantially boost the acceleration and distribute available electric power to maximize torque according to the road grip conditions and weight transfer in the car.
- Multiphysics analysis of multi-port electrical machines and systems with an emphasis on structural reliability (especially for machines with DMP feature or multi-DOF machines), thermal design and electromagnetic compatibility design of associated drives. With the increase of the number of electrical and/or mechanical ports, the redundancy of electrical or mechanical components and the possibility of coupling among different components or multiple fields increase accordingly, which calls for more elaborated coupling analysis. The indirect coupling between

two stator windings of BDFMs mentioned in Section II-C and the cooling system design of DEP+DMP machines mentioned in Section IV are good examples.

- New methods and tools for modeling, analysis and control of multi-port machines and systems. There is still a long way to go before multi-port electrical machines and systems grow as mature as the conventional single-input single-output counterparts. This might be primarily caused by higher system machine complexity and more diversified application needs. For instance, the spiral vector theory unifies the steady-state and dynamic analysis, thus may model multi-port electrical machine more effectively [55]. The general airgap field modulation theory may offer a new way for a better understanding of the working mechanism of multi-port machines [26]. Moreover, multi-port machines usually require unconventional converter topologies or flexible configurations of standard power converters, so the control schemes and/or pulse width modulation strategies for conventional machines will have to be extended or modified to well suit corresponding multi-port systems.

REFERENCES

[1] A. E. Fitzgerald, C. Kingsley, Jr. and S. D. Jmans, "Electromechanical-energy-conversion principles" in *Electric Machinery*, 6 ed, McGraw-Hill, 2003.

[2] L. Xu, "A new breed of electric machines-basic analysis and applications of dual mechanical port electric machines," in *Proc. Int. Conf. Electr. Mach. Syst.* (*ICEMS*), pp. 24-31, Sep. 2005, doi: 10.1109/ICEMS.2005.202477.

[3] R. Cardenas, R. Pena, S. Alepuz and G. Asher, "Overview of control systems for the operation of DFIGs in wind energy applications," *IEEE Trans. Ind. Electron.*, vol. 60, no. 7, pp. 2776-2798, Jan. 2013, doi: 10.1109/TIE.2013.2243372.

[4] S. Basak and C. Chakraborty, "Dual stator winding induction machine: problems, progress, and future scope," *IEEE Trans. Ind. Electron*., vol. 62, no. 7, pp. 4641-4652, Jul. 2015, doi: 10.1109/TIE.2015.2409800.

[5] T. D. Strous, H. Polinder and J. A. Ferreira, "Brushless doubly-fed induction machines for wind turbines: developments and research challenges," *IET Electric. Power Appl*., vol. 11, no. 6, pp. 991-1000, Jul. 2017, doi: 10.1049/iet-epa.2016.0118.

[6] P. L. Alger, E. H. Freiburghouse and D. D. Chase, "Double windings for turbine alternators," *Trans. AIEE*, vol. 49, no. 1, pp. 226-244, Jan. 1930, doi: 10.1109/JAIEE.1930.6538560.

[7] P. W. Franklin, "A theoretical study of the three phase salient pole type generator with simultaneous ac and bridge rectified dc output-Part I," *IEEE Trans. Power Apparat. Syst*., vol. PAS-92, no. 2, pp. 543-551, Mar. 1973, doi: 10.1109/TPAS.1973.293755.

[8] R. H. Nelson and P. C. Krause, "Induction machine analysis for arbitrary displacement between multiple winding sets," *IEEE Trans. Power Apparat. Syst.*, vol. PAS-93, no. 3, pp. 841-848, May 1974, doi: 10.1109/TPAS.1974.293983.

[9] J.-R. Fu and T. A. Lipo, "Disturbance-free operation of a multiphase current-regulated motor drive with an opened phase," *IEEE Trans. Ind. Appl.*, vol. 30, no. 5, pp. 1267-1274, Sep./Oct. 1994, doi: 10.1109/28.315238.

[10] R. O. C. Lyra and T. A. Lipo, "Torque density improvement in a six-phase induction motor with third harmonic current injection," *IEEE Trans. Ind. Appl*., vol. 38, no. 5, pp. 1351-1360, Sep./Oct. 2002, doi: 10.1109/TIA.2002.802938.

[11] J. C. Prescott and B. P. Raju, "The inherent instability of induction motors under conditions of double supply," *Proc. IEE-Part C: Monographs*, vol. 105, no. 7, pp. 319-329, Mar. 1958, doi: 10.1049/pi-c.1958.0040.

[12] B. H. Smith, "Synchronous behavior of doubly fed twin stator induction machine," *IEEE Trans. Power Apparat. Syst*., vol. PAS-86, no. 10, pp. 1227-1236, Oct. 1967, doi: 10.1109/TPAS.1967.291897.

[13] A. R. W. Broadway and L. Burbridge, "Self-cascaded machine: a low-speed motor or high-frequency brushless alternator," *Proc. IEE*, vol. 117, no. 7, pp. 1277-1290, Jul. 1970, doi: 10.1049/piee.1970.0247.

[14] A. R. W. Broadway, "Cageless induction machine," *Proc. IEE*, vol. 118, no. 11, pp. 1593-1600, Nov. 1971, doi: 10.1049/piee.1971.0290.

[15] S. Eriksson and C. Sadarangani, "A four-quadrant HEV drive system," in *Proc. Veh. Technol. Conf.* (*VTC*), pp. 1510-1514, Sep. 2002, doi: 10.1109/VETECF.2002.1040468.

[16] M. J. Hoeijmakers and M. Rondel, "The electrical variable transmission in a city bus," in *Proc. Power Electron. Special. Conf.* (*PESC*), pp. 2773-2778, Jun. 2004, doi: 10.1109/PESC.2004.1355272.

[17] H. Akagi and H. Sato, "Control and performance of a doubly-fed induction machine intended for a flywheel energy storage system," *IEEE Trans. Power Electron*., vol. 17, no. 1, pp. 109-116, Jan. 2002, doi: 10.1109/63.988676.

[18] A. Banerjee, M. S. Tomovich, S. B. Leeb and J. L. Kirtley, "Power converter sizing for a switched doubly fed machine propulsion drive," *IEEE Trans. Ind.*, vol. 51, no. 1, pp. 248-258, Jan./Feb. 2015, doi: 10.1109/TIA.2014.2330074.

[19] A. Banerjee, S. B. Leeb and J. L. Kirtley, "Seamless grid interaction for a switched doubly-fed machine propulsion drive," in *Proc. Int. Electr. Mach. Drives Conf.* (*IEMDC*), pp. 1049-1055, May 2015, doi: 10.1109/IEMDC.2015.7409191.

[20] A. Banerjee, S. B. Leeb and J. L. Kirtley, "Solid-state transfer switch topologies for a switched doubly fed machine drive," *IEEE Trans. Power Electron.*, vol. 31, no. 8, pp. 5709-5720, Oct. 2015, doi: 10.1109/TPEL.2015.2489463.

[21] L. Morel, H. Godfroid, A. Mirzaian and J.-M. Kauffmann, "Double-fed induction machine: converter optimisation and field oriented control without position sensor," *IEE Proc. Electr. Power Appl.*, vol. 145, no. 4, pp. 360-368, Jul. 1998, doi: 10.1049/ip-epa:19981982.

[22] A. Banerjee, A. H. Chang, K. Surakitbovorn, S. B. Leeb and J. L. Kirtley, "Switched doubly-fed machine propulsion drive," in *Proc. IEEE Appl. Power Electron. Conf. Expo*. (*APEC*), pp. 775-782, Mar. 2014, doi: 10.1109/APEC.2014.6803396.

[23] A. Banerjee, S. B. Leeb and J. L. Kirtley, "A comparison of switched doubly-fed machine drive topologies for high power applications," in *Proc. IEEE Int. Electr. Mach. Drives Conf.* (*IEMDC*), pp. 796-803, May 2015, doi: 10.1109/IEMDC.2015.7409151.

[24] M. Abdellatif, M. Debbou, I. Slama-Belkhodja and M. Pietrzak-David, "Simple low-speed sensorless dual DTC for double fed induction machine drive," *IEEE Trans. Ind. Electron*., vol. 61, no. 8, pp. 3915-3922, Aug. 2014, doi: 10.1109/TIE.2013.2288190.

[25] Y. Liu and L. Xu, "The dual-current-loop controlled doubly fed induction motor for EV/HEV applications," *IEEE Trans. Energy Convers*., vol. 28, no. 4, pp. 1045-1052, Dec. 2013, doi: 10.1109/TEC.2013.2279853.

[26] M. Cheng, P. Han and W. Hua, "General airgap field modulation theory for electrical machines," *IEEE Trans. Ind. Electron.*, vol. 64, no. 8, pp. 6063-6074, Aug. 2017, doi: 10.1109/TIE.2017.2682792.

[27] W. N. W. A. Munim, M. J. Duran, H. S. Che, M. Bermudez, I. G.-Prieto and N. A. Rahim, "A unified analysis of the fault tolerance capability in six-phase induction motor drives," *IEEE Trans. Power Electron*., vol. 32, no. 10, pp. 7824-7836, Oct. 2017, doi: 10.1109/TPEL.2016.2632118.

[28] R. Bojoi, M. Lazzari, F. Profumo and A. Tenconi, "Digital field-oriented control for dual three-phase induction motor drives," *IEEE Trans. Ind. Appl.*, vol. 39, no. 3, pp. 752-760, May/Jun. 2003, doi: 10.1109/TIA.2003.811790.

[29] A. Boglietti, R. Bojoi, A. Cavagnino and A. Tenconi, "Efficiency analysis of PWM inverter fed three-phase and dual three-phase high frequency induction machines for low/medium power applications," *IEEE Trans. Ind. Electron*., vol. 55, no. 5, pp. 2015-2023, May 2005, doi: 10.1109/TIE.2008.918489.

[30] L. Alberti and N. Bianchi, "Experimental tests of dual three-phase induction motor under faulty operating condition," *IEEE Trans. Ind. Electron*., vol. 59, no. 5, pp. 2041-2048, May 2012, doi: 10.1109/TIE.2011.2171175.

[31] H. S. Che, E. Levi, M. Jones, M. J. Duran, W. P. Hew and N. A. Rahim, "Operation of a six-phase induction machine using series-connected machine-side converters," *IEEE Trans. Ind. Electron*., vol. 61, no. 1, pp. 164-176, Jan. 2014, doi: 10.1109/TIE.2013.2248338.

[32] F. Bu, W. Huang, Y. Hu and K. Shi, "An integrated ac and dc hybrid generation system using dual-stator-winding induction generator with static excitation controller," *IEEE Trans. Energy Convers*., vol. 27, no. 3, pp. 810-812, Sep. 2012, doi: 10.1109/TEC.2012.2203956.

[33] H. S. Che, M. J. Duran, E. Levi, M. Jones, W. P. Hew and N. A. Rahim, "Postfault operation of an asymmetrical six-phase induction machine with single and two isolated neutral points," *IEEE Trans. Power Electron*., vol. 29, no. 10, pp. 5406-5416, Jul. 2014, doi: 10.1109/TPEL.2013.2293195.

[34] M. J. Duran, I. Gonzalez-Prieto, M. Bermudez, F. Barrero, H. Guzman and M. R. Arahal, "Optimal fault-tolerant control of six-phase induction motor drives with parallel converters," *IEEE Trans. Ind. Electron*., vol. 63, no. 1, pp. 629-640, Jan. 2016, doi: 10.1109/TIE.2015.2461516.

[35] I. Gonzalez-Prieto, M. J. Duran, H. S. Che, E. Levi, M. Bermudez and F. Barrero, "Fault-tolerant operation of six-phase energy conversion systems with parallel machine-side converters," *IEEE Trans. Power Electron*., vol. 31, no. 4, pp. 3068-3079, Apr. 2016, doi: 10.1109/TPEL.2015.2455595.

[36] I. Gonzalez-Prieto, M. J. Duran, F. Barrero, M. Bermudez and H. Guzman, "Impact of post-fault flux adaptation on six-phase induction motor drives with parallel converters," *IEEE Trans. Power Electron*., vol. 33, no. 1, pp. 515-528, Jan. 2017, doi: 10.1109/TPEL.2016.2533719.

[37] R. Kianinezhad, B. Nahid-Mobarakeh, L. Baghli, F. Betin and G.-A. Capolino, "Modeling and control of six-phase symmetrical induction machine under fault condition due to open phases," *IEEE Trans. Ind. Electron*., vol. 55, no. 5, pp. 1966-1977, May 2008, doi: 10.1109/TIE.2008.918479.

[38] H. S. Che and W. P. Hew, "Dual three-phase operation of single neutral symmetrical six-phase machine for improved performance," in *Proc. Annu. Conf. Ind. Electron. Soc*. (*IECON*), Yokohama, Japan, 9-12 Nov. 2015, doi: 10.1109/IECON.2015.7392259.

[39] I. Subotic, N. Bodo, E. Levi, M. Jones and V. Levi, "Isolated chargers for EVs incorporating six-phase machines," *IEEE Trans. Ind. Electron*., vol. 63, no. 1, pp. 653-664, Jan. 2016, doi: 10.1109/TIE.2015.2412516.

[40] Y. Li, Y. Hu, W. Huang, L. Liu and Y. Zhang, "The capacity optimization for the static excitation controller of the dual-stator-winding induction generator operating in a wind speed range," *IEEE Trans. Ind. Electron*, vol. 56, no. 2, pp. 530-541, Feb. 2009, doi: 10.1109/TIE.2008.2003363.

[41] F. Bu, W. Huang, Y. Hu, J. Shi and K. Shi, "A stand-alone dual stator-winding induction generator variable frequency ac power system," *IEEE Trans. Power Electron*., vol. 27, no. 1, pp. 10-13, Jan. 2012, doi: 10.1109/TPEL.2011.2157170.

[42] A. R. Munoz and T. A. Lipo, "Dual stator winding induction machine drive," *IEEE Trans. Ind. Appl*., vol. 36, no. 5, pp. 1369-1379, Sep./Oct. 2000, doi: 10.1109/28.871286.

[43] Z. Wu, O. Ojo and J. Sastry, "High-performance control of a dual stator winding dc power induction generator," *IEEE Trans. Ind. Appl*., vol. 43, no. 2, pp. 582-592, Mar./Apr. 2007, doi: 10.1109/TIA.2006.890020.

[44] M. Barcaro, N. Bianchi and F. Magnussen, "Faulty operations of a PM fractional-slot machine with a dual three-phase winding," *IEEE Trans. Ind. Electron.*, vol. 58, no. 9, pp. 3825-3832, Sep. 2011, doi: 10.1109/TIE.2010.2087300.

[45] Y. Zhou, X. Lin and M. Cheng, "A fault-tolerant direct torque control for six-phase permanent magnet synchronous motor with arbitrary two opened phases based on modified variables," *IEEE Trans. Energy Convers*., vol. 31, no. 2, pp. 549-556, Jun. 2016, doi: 10.1109/TEC.2015.2504376.

[46] Z. Wang, X. Wang, J. Cao, M. Cheng and Y. Hu, "Direct torque control of T-NPC inverters fed double-stator-winding PMSM drives with SVM," *IEEE Trans. Power Electron*., DOI: 10.1109/TPEL.2017.2689008.

[47] E. S. Obe and T. Senjyu, "Analysis of a polyphase synchronous reluctance motor with two identical stator windings," *Electr. Power Syst. Res.*, vol. 76, no. 6-7, pp. 515-524, Apr. 2006, doi: 10.1016/j.epsr.2005.07.004.

[48] W. Ding, Y. Hu and L. Wu, "Investigation and experimental test of fault-tolerant operation of a mutually coupled dual three-phase SRM drive under faulty conditions," *IEEE Trans. Power Electron*., vol. 30, no. 12, pp. 6857-6872, Dec. 2015, doi: 10.1109/TPEL.2015.2389258.

[49] M. Ruviaro, F. Runcos, N. Sadowski and I. M. Borges, "Analysis and tests results of a brushless doubly-fed induction machine with rotary transformer," *IEEE Trans. Ind. Electron*., vol. 59, no. 6, pp. 2670-2677, Jun. 2012, doi: 10.1109/TIE.2011.2165457.

[50] N. ur Rehman Malik and C. Sadarangani, "Brushless doubly-fed induction machine with rotating power electronic converter for wind power applications," in *Proc. Int. Conf. Electr. Mach. Syst.* (*ICEMS*), pp.1-6, Aug. 2011, doi: 10.1109/ICEMS.2011.6073422.

[51] Y. Liao, L. Xu and L. Zhen, "Design of a doubly fed reluctance motor for adjustable-speed drives," *IEEE Trans. Ind. Appl*., vol. 32, no. 5, pp. 1195-1203, Sep./Oct. 1996, doi: 10.1109/28.536883.

[52] K. Protsenko and D. Xu, "Modeling and control of brushless doubly fed induction generators in wind energy applications," *IEEE Trans. Power Electron*., vol. 23, no. 3, pp. 1191-1197, May 2008, doi: 10.1109/TPEL.2008.921187.

[53] J. Poza, E. Oyarbide, I. Sarasola and M. Rodriguez, "Vector control design and experimental evaluation for the brushless doubly fed machine," *IET Proc.-Electr. Power Appl*., vol. 3, no. 4, pp. 247-256, Jul. 2009, doi: 10.1049/iet-epa.2008.0090.

[54] S. Ademi and M. G. Jovanovic, "Vector control methods for brushless doubly fed reluctance machines," *IEEE Trans. Ind. Electron*., vol. 62, no. 1, pp. 96-104, Jan. 2015, doi: 10.1109/TIE.2014.2327564.

[55] P. Han, M. Cheng, X. Wei and N. Li, "Modeling and performance analysis of a dual-stator brushless doubly fed induction machine based on spiral vector theory," *IEEE Trans. Ind. Appl*., vol. 52, no. 2, pp. 1380-1389, Mar./Apr. 2016, doi: 10.1109/TIA.2015.2491893.

[56] P. Han, M. Cheng, X. Wei and Y. Jiang, "Steady-state characteristics of the dual-stator brushless doubly-fed induction generator," *IEEE Trans. Ind. Electron*., doi: 10.1109/TIE.2017.2716904.

[57] S. Shao, T. Long, E. Abdi and R. A. McMahon, "Dynamic control of the brushless doubly fed induction generator under unbalanced operation," *IEEE Trans. Ind. Electron*., vol. 60, no. 6, pp. 2465-2476, Jun. 2013, doi: 10.1109/TIE.2012.2211313.

[58] P. Han, M. Cheng, Y. Jiang and Z. Chen, "Torque/power density optimization of a dual-stator brushless doubly-fed induction generator for wind power application," *IEEE Trans. Ind. Electron*., vol. 64, no. 12, pp. 9864-9875, Dec. 2017, doi: 10.1109/TIE.2017.2726964.

[59] M. Cheng, P. Han and X. Wei, "Design, analysis and control of brushless doubly-fed generators for wind power application," *Trans. China Electrotech. Soc*., vol. 31, no. 19, pp. 37-53, Oct. 2016.

[60] A. M. Knight, R. E. Betz and D. G. Dorrell, "Design and analysis of brushless doubly fed reluctance machines," *IEEE Trans. Ind. Appl*., vol. 49, no. 1, pp. 50-58, Jan./Feb. 2013, doi: 10.1109/TIA.2012.2229451.

[61] P. Han, M. Cheng, X. Zhu and Z. Chen, "Multifrequency spiral vector model for the brushless doubly-fed induction machine," in *Proc. IEEE Int. Electr. Mach. Drives Conf.* (*IEMDC*), pp. 1-8, May 2017, doi: 10.1109/IEMDC.2017.8002129.

[62] F. Xiong and X. Wang, "Design of a low-harmonic-content wound rotor for the brushless doubly fed generator," *IEEE Trans. Energy Convers*., vol. 29, no. 1, pp. 158-168, Mar. 2014, doi: 10.1109/TEC.2013.2287908.

[63] F. Zhang, G. Jia, Y. Zhao, Z. Yang, W. Cao and J. L. Kirtley, "Simulation and experimental analysis of a brushless electrically excited synchronous machine with hybrid rotor," *IEEE Trans. Magn*., vol. 51, no. 12, Dec. 2015, Article #: 8115007, doi: 10.1109/TMAG.2015.2450684.

[64] P. Han, M. Cheng and R. Luo, "Design and analysis of a brushless doubly-fed induction machine with dual-stator structure," *IEEE Trans. Energy Convers.*, vol. 31, no. 3, pp. 1132-1141, Sep. 2016, doi: 10.1109/TEC.2016.2547955.

[65] T. Fukami, M. Momiyama and K. Shima, "Steady-state analysis of a dual-winding reluctance generator with a multiple-barrier rotor," *IEEE Trans. Energy Convers*., vol. 23, no. 2, pp.492-498, Jun. 2008, doi: 10.1109/TEC.2008.918656.

[66] M. Hashemnia, F. Tahami and E. Oyarbide, "Investigation of core loss effect on steady-state characteristics of inverter fed brushless doubly fed machines," *IEEE Trans. Energy Convers*., vol. 29, no. 1, pp. 57-64, Mar. 2014, doi: 10.1109/TEC.2013.2290428.

[67] H. Gorginpour, H. Oraee and E. Abdi, "Calculation of core and stray load losses in brushless doubly fed induction generators," *IEEE Trans. Ind. Electron.*, vol. 61, no. 7, pp. 3167-3177, Jul. 2014, doi: 10.1109/TIE.2013.2279357.

[68] T. D. Strous, X. Wang, H. Polinder and J. A. Ferreira, "Brushless doubly fed induction machines: magnetic field analysis," *IEEE Trans. Magn.*, vol. 52, no. 11, Nov. 2016, Article#: 8108310, doi: 10.1109/TMAG.2016.2587879.

[69] S. Abdi, E. Abdi, A. Oraee and R. McMahon, "Optimization of magnetic circuit for brushless doubly fed machines," *IEEE Trans. Energy Convers*., vol. 33, no. 4, pp. 1611-1620, Dec. 2015, doi: 10.1109/TEC.2015.2468063.

[70] H. Gorginpour, H. Oraee and R. A. McMahon, "Electromagnetic-thermal design optimization of the brushless doubly fed induction generator," *IEEE Trans. Ind. Electron*., vol. 61, no. 4, pp. 1710-1721, Apr. 2014, doi: 10.1109/TIE.2013.2267705.

[71] X. Wang, T. D. Strous, D. Lahaye, H. Polinder and J. A. Ferreira, "Modeling and optimization of brushless doubly-fed induction machines using computationally efficient finite-element analysis," *IEEE Trans. Ind.*

Appl., vol. 52, no. 6, pp. 4525-4534, Nov./Dec. 2016, doi: 10.1109/TIA.2016.2593715.

[72] S. Shao, E. Abdi, F. Barati and R. McMahon, "Stator-flux-oriented vector control for brushless doubly fed induction generator," *IEEE Trans. Ind. Electron.*, vol. 56, no. 10, pp. 4220-4228, Oct. 2009, doi: 10.1109/TIE.2009.2024660.

[73] P. C. Roberts, T. Long, R. A. McMahon and S. Shao, "Dynamic modelling of the brushless doubly fed machine," *IET Proc.-Electr. Power Appl*., vol. 7, no. 7, pp. 544-556, Aug. 2013, doi: 10.1049/iet-epa.2012.0293.

[74] F. Barati, R. McMahon, S. Shao, E. Abdi and H. Oraee, "Generalized vector control for brushless doubly fed machines with nested-loop rotor," *IEEE Trans. Ind. Electron*., vol. 60, no. 6, pp. 2477-2485, Jun. 2013, doi: 10.1109/TIE.2012.2226415.

[75] A. Zhang, X. Wang, W. Jia and Y. Ma, "Indirect stator-quantities control for the brushless doubly fed induction machine," *IEEE Trans. Power Electron.*, vol. 29, no. 3, pp. 1392-1401, Mar. 2014, doi: 10.1109/TPEL.2013.2260870.

[76] P. Han, M. Cheng and Zhe Chen, "Single-electrical-port control of cascaded doubly-fed induction machine for EV/HEV applications," *IEEE Trans. Power Electron*., vol. 32, no. 9, pp. 7233-7243, Sep. 2017, doi: 10.1109/TPEL.2016.2623247.

[77] P. Han, M. Cheng and Z. Chen, "Dual-electrical-port control of cascaded brushless doubly-fed induction drive for EV/HEV applications," *IEEE Trans. Ind. Appl*., vol. 53, no. 2, pp.1390-1398, Mar./Apr. 2017, doi: 10.1109/TIA.2016.2625770.

[78] S. Jin, L. Shi, L. Zhu, W. Cao, T. Dong and F. Zhang, "Dual two-level converters based on direct power control for an open-winding brushless doubly-fed reluctance generator," *IEEE Trans. Ind. Appl*., vol. 53, no. 4, pp. 3898-3906, Jul./Aug. 2017, doi: 10.1109/TIA.2017.2693959.

[79] G. Esfandiari, M. Ebrahimi and A. Tabesh, "Instantaneous torque control method with rated torque sharing ratio for cascaded DFIMs," *IEEE Trans. Power Electron*., vol. 32, no. 11, pp. 8671-8680, Nov. 2017, doi: 10.1109/TPEL.2017.2650211.

[80] G. Zhang, J. Yang, Y. Sun, M. Su, W. Tang, Q. Zhu, et al. "A robust control scheme based on ISMC for the BDFIM," *IEEE Trans. Power Electron*., doi: 10.1109/TPEL.2017.2708741.

[81] X. Wei, M. Cheng, W. Wang, P. Han and R. Luo, "Direct voltage control of dual-stator brushless doubly-fed induction generator for stand-alone wind energy conversion systems," *IEEE Trans. Magn*., vol. 52, no. 7, Jul. 2016, Article #: 8203804, doi: 10.1109/TMAG.2016.2526049.

[82] X. Wang, H. Lin and Z. Wang, "Transient control of the reactive current for the line-side converter of the brushless doubly-fed induction generator in stand-alone operation," *IEEE Trans. Power Electron*., vol. 32, no. 10, pp. 8193-8203, Oct. 2017, doi: 10.1109/TPEL.2016.2609461.

[83] L. Sun, Y. Chen, J. Su, D. Zhang, L. Peng and Y. Kang, "Decoupling network design for inner current loops of stand-alone brushless doubly fed induction generation power system," *IEEE Trans. Power Electron*., doi: 10.1109/TPEL.2017.2734108.

[84] I. A. Gowaid, A. S. Abdel-Khalik, A. M. Massoud and S. Ahmed, "Ride-through capability of grid-connected brushless cascade DFIM wind turbines in faulty grid conditions - a comparative study," *IEEE Trans. Sustain. Energy*, vol. 4, no. 4, pp. 1002-1015, Oct. 2013, doi: 10.1109/TSTE.2013.2261830.

[85] T. Long, S. Shao, P. Malliband and E. Abdi, "Crowbarless fault ride-through of the brushless doubly fed induction generator in a wind turbine under symmetrical voltage dips," *IEEE Trans. Ind. Electron*., vol. 60, no. 7, pp. 2833-2841, Jul. 2013, doi: 10.1109/TIE.2012.2208437.

[86] T. Long, S. Shao, E. Abdi and R. A. McMahon, "Asymmetrical low-voltage ride through of brushless doubly fed induction generators for the wind power generation," *IEEE Trans. Energy Convers*., vol. 28, no. 3, pp. 502-511, Sep. 2013, doi: 10.1109/TEC.2013.2261818.

[87] J. Hu, J. Zhu and D. G. Dorrell, "A new control method of cascaded brushless doubly fed induction generators using direct power control," *IEEE Trans. Energy Convers*., vol. 29, no. 3, pp. 771-779, Jun. 2014, doi: 10.1109/TEC.2014.2325046.

[88] J. Chen, W. Zhang, B. Chen and Y. Ma, "Improved vector control of brushless doubly fed induction generator under unbalanced grid conditions for offshore wind power generations," *IEEE Trans. Energy Convers*., vol. 31, no. 1, pp. 293-302, Mar. 2016, doi: 10.1109/TEC.2015.2479859.

[89] M. G. Jovanovic, J. Yu and E. Levi, "Encoderless direct torque controller for limited speed range applications of brushless doubly fed reluctance motors," *IEEE Trans. Ind. Appl*., vol. 42, no. 3, pp. 712-722, May/Jun. 2006, doi: 10.1109/TIA.2006.872955.

[90] H. Chaal and M. Jovanovic, "Practical implementation of sensorless torque and reactive power control of doubly-fed machines," *IEEE Trans. Ind. Electron.*, vol. 59, no. 6, pp. 2645-2653, Jun. 2012, doi: 10.1109/TIE.2011.2161065.

[91] S. Ademi, M. Jovanovic and H. Chaal, "A new sensorless speed control scheme for doubly fed reluctance generators," *IEEE Trans. Energy Convers*., vol. 31, no. 3, pp. 993-1001, Sep. 2016, doi: 10.1109/TEC.2016.2533609.

[92] U. Shipurkar, T. D. Strous, H. Polinder, J. A. Ferreira and A. Veltman, "Achieving sensorless control for the brushless doubly-fed induction machine," *IEEE Trans. Energy Convers*., doi: 10.1109/TEC.2017.2724204.

[93] J. F. H. Douglas, "Characteristics of induction motors with permanent magnet excitation," *Trans. AIEE. Power Appl. Syst.*, vol. 78, no. 3, pp. 221-225, Apr. 1959, doi: 10.1109/AIEEPAS.1959.4500298.

[94] G. Gail, T. Harkopf, E. Troster, M. Hoffling, M. Henschel and H. Schneider, "Static and dynamic measurements of a permanent magnet induction generator: test results of a new generator concept," in *Proc. Int. Conf. Electr. Mach.* (*ICEM*), Cracow, Poland, Sep. 2004, pp. 666-671.

[95] T. Fukami, K. Nakagawa, Y. Kanamaru and T. Miyamoto, "A technique for the steady-state analysis of a grid-connected permanent-magnet induction generator," *IEEE Trans. Energy Convers*., vol. 19, no. 2, pp. 318-324, Jun. 2004, doi: 10.1109/TEC.2004.827009.

[96] T. Tsuda, T. Fukami, Y. Kanamaru and T. Miyamoto, "Effects of the built-in permanent magnet rotor on the equivalent circuit parameters of a permanent magnet induction generator," *IEEE Trans. Energy Convers*., vol. 22, no. 3, pp. 798-799, Sep. 2007, doi: 10.1109/TEC.2007.902674.

[97] J. H. J. Potgieter and M. Kamper, "Design of new concept direct grid-connected slip-synchronous permanent-magnet wind generator," *IEEE Trans. Ind. Appl*., vol. 48, no. 3, pp. 913-922, May/Jun. 2012, doi: 10.1109/TIA.2012.2191251.

[98] R. Qu and T. A. Lipo, "Dual-rotor, radial-flux, toroidally wound, permanent-magnet machines," *IEEE Trans. Ind. Appl*., vol. 39, no. 6, pp. 1665-1673, Nov.-Dec. 2003, doi: 10.1109/TIA.2004.827444.

[99] T. Zou, D. Li, R. Qu, J. Li and D. Jiang, "Analysis of a dual-rotor, toroidal-winding, axial-flux vernier permanent magnet machine," *IEEE Trans. Ind. Appl*., vol. 53, no. 3, pp. 1920-1930, May/Jun. 2017, doi: 10.1109/TIA.2017.2657493.

[100] R. Madhavan and B. G. Fernandes, "Axial flux segmented SRM with a higher number of rotor segments for electric vehicles," *IEEE Trans. Energy Convers*., vol. 28, no. 1, pp. 203-213, Mar. 2013, doi: 10.1109/TEC.2012.2235068.

[101] M. Venturini and F. Leonardi, "High torque, low speed joint actuator based on PM brushless motor and magnetic gearing," in *Rec. IEEE IAS Annu. Meeting*, pp. 37-42, Oct. 1993, doi: 10.1109/IAS.1993.298900.

[102] L. Jian, K. T. Chau and J. Z. Jiang, "A magnetic-geared outer-rotor permanent-magnet brushless machine for wind power generation," *IEEE Trans. Ind. Appl.*, vol. 45, no. 3, pp. 954-962, May/Jun. 2009, doi: 10.1109/TIA.2009.2018974.

[103] P. O. Rasmussen, H. H. Mortensen, T. N. Matzen, T. M. Jahns and H. A. Toliyat, "Motor integrated permanent magnet gear with a wide torque-speed range," in *Proc. Energy Convers. Congr. Expo.* (*ECCE*), pp. 1510-1518, Sep. 2009, doi: 10.1109/ECCE.2009.5316280.

[104] K. Atallah, J. Rens, S. Mezani and D. Howe, "A novel "pseudo" direct-drive brushless permanent magnet machine," *IEEE Trans. Magn*., vol. 44, no. 11, pp. 4349-4352, Nov. 2008, doi: 10.1109/TMAG.2008.2001509.

[105] T. V. Frandsen, P. O. Rasmussen and K. K. Jensen, "Improved motor integrated permanent magnet gear for traction applications," in *Proc. IEEE Energy Convers. Congr. Expo.* (*ECCE*), pp. 3332-3339, Sep. 2012, doi: 10.1109/ECCE.2012.6342334.

[106] T. V. Frandsen, L. Mathe, N. I. Berg, R. K. Holm, T. N. Matzen, P. O. Rasmussen, et al. "Motor integrated permanent magnet gear in a battery electrical vehicle," *IEEE Trans. Ind. Appl.*, vol. 51, no. 2, Mar./Apr. 2015, doi: 10.1109/TIA.2014.2360016.

[107] J. Bai, P. Zheng, C. Tong, Z. Song and Q. Zhao, "Characteristic analysis and verification of the magnetic-field-modulated brushless double-rotor machine," *IEEE Trans. Ind. Electron*., vol. 62, no. 7, pp. 4023-4033, Jul. 2015, doi: 10.1109/TIE.2014.2381159.

[108] L. Sun, M. Cheng, H. Wen and L. Song, "Motion control and performance evaluation of a magnetic-geared dual-rotor motor in hybrid powertrain,"

IEEE Trans. Ind. Electron., vol. 64, no. 3, pp. 1863-1872, Mar. 2017, doi: 10.1109/TIE.2016.2627018.

[109] L. Sun, M. Cheng, J. Zhang and L. Song, "Analysis and control of complementary magnetic-geared dual-rotor motor," *IEEE Trans. Ind. Electron*., vol. 63, no. 11, pp. 6715-6725, Nov. 2016, doi: 10.1109/TIE.2016.2581768.

[110] L. Sun, M. Cheng and M. Tong, "Key issues in design and manufacture of magnetic-geared dual-rotor motor for hybrid vehicles," *IEEE Trans. Energy Convers.*, doi: 10.1109/TEC.2017.2697758.

[111] M. Fukuoka, K. Nakamura, H. Kato and O. Ichinokura, "A novel flux-modulated type dual-axis motor for hybrid electric vehicles," *IEEE Trans. Magn*., vol. 50, no. 11, Nov. 2014, Article#: 8202804, doi: 10.1109/TMAG.2014.2327646.

[112] G. T. Rodenhuis, "Dynamoelectric gear," EP Patent 1154551 A2, Jan. 2000.

[113] Y. Liu, D. Cheng, Y. Sui, J. Bai, C. Tong and W. Tong, "Magnetic system study of a compound-structure permanent-magnet synchronous machine for HEVs," *IEEE Trans. Ind. Appl*., vol. 48, no. 6, pp. 1797-1807, Nov./Dec. 2012, doi: 10.1109/TIA.2012.2221451.

[114] H. Cai and L. Xu, "Modeling and control for cage rotor dual mechanical port electric machine-part II: independent control of two rotors," *IEEE Trans. Energy Convers.*, vol. 30, no. 3, pp. 966-973, Sep. 2015, doi: 10.1109/TEC.2015.2400971.

[115] J. Druant, F. D. Belie, P. Sergant and J. Melkebeek, "Field-oriented control for an induction-machine-based electrical variable transmission," *IEEE Trans. Veh. Technol.*, vol. 65, no. 6, pp. 4230-4240, Jun. 2016, doi: 10.1109/TVT.2015.2496625.

[116] J. Druant, F. D. Belie, J. Melkebeek and P. Sergeant, "Torque analysis on a double rotor electrical variable transmission with hybrid excitation," *IEEE Trans. Ind. Electron*., vol. 64, no. 1, pp. 60-68, Jan. 2017, doi: 10.1109/TIE.2016.2608768.

[117] T. Guo, N. Schofield and A. Emadi, "Double segmented rotor switched reluctance machine with shared stator back-iron for magnetic flux passage," *IEEE Trans. Energy Convers*., vol. 31, no. 4, pp. 1278-1286, Dec. 2016, doi: 10.1109/TEC.2016.2600178.

[118] L. Xu, Y. Zhang and X. Wen, "Multioperational modes and control strategies of dual-mechanical-port machine for hybrid electrical vehicles," *IEEE Trans. Ind. Appl*., vol. 45, no. 2, pp. 747-755, Mar./Apr. 2009, doi: 10.1109/TIA.2009.2013575.

[119] P. Zheng, E. Nordlund, P. Thelin and C. Sadarangani, "Investigation of the winding current distribution in a 4-quadrant-transducer prototype machine," *IEEE Trans. Magn*., vol. 41, no. 5, pp. 1972-1975, May 2005, doi: 10.1109/TMAG.2005.846279.

[120] P. Zheng, R. Liu, P. Thelin, E. Nordlund and C. Sadarangani, "Research on the cooling system of a 4QT prototype machine used for HEV," *IEEE Trans. Energy Convers.*, vol. 23, no. 1, pp. 61-67, Mar. 2008, doi: 10.1109/TEC.2007.914356.

[121] X. Sun and M. Cheng, "Thermal analysis and cooling system design of dual mechanical port machine for wind power application," *IEEE Trans. Ind. Electron.*, vol. 60, no. 5, pp. 1724-1733, May 2013, doi: 10.1109/TIE.2012.2190958.

[122] S. Zhu, M. Cheng and X. Sun, "Mechanical design of outer-rotor structure for dual mechanical port machine," in *Proc. Int. Conf. Electr. Mach. Syst.* (*ICEMS*), pp. 1-6, Aug. 2011, doi: 10.1109/ICEMS.2011.6073873.

[123] X. Sun, M. Cheng, S. Zhu and J. Zhang, "Coupled electromagnetic-thermal-mechanical analysis for accurate prediction of dual-mechanical-port machine performance," *IEEE Trans. Ind. Appl*., vol. 48, no. 6, pp. 2240-2248, Nov./Dec. 2012, doi: 10.1109/TIA.2012.2226859.

[124] Y. Cheng, R. Trigui, C. Espanet, A. Bouscayrol and S. Cui, "Specifications and design of a PM electric variable transmission for toyota prius II," *IEEE Trans. Veh. Technol.*, vol. 60, no. 9, pp. 4106-4114, Nov. 2011, vol. 10.1109/TVT.2011.2155106.

[125] E. Vinot, R. Trigui, Y. Cheng, C. Espanet, A. Bouscayrol and V. Reinbold, "Improvement of an EVT-based HEV using dynamic programming" *IEEE Trans. Veh. Technol.*, vol. 63, no. 1, pp. 40-50, Jan. 2014, doi: 10.1109/TVT.2013.2271646.

[126] T. Watanabe, E. Tsuchiya, M. Ebina and Y. Osada, "High efficiency electromagnetic torque converter for hybrid electric vehicles," *SAE Int. J. Alt. Power*., vol. 5, no. 2, pp. 228-236, 2016. doi: 10.4271/2016-01-1162.

[127] Y. Yeh, M. Hsieh and D. G. Dorrell, "Different arrangements for dual-rotor dual-output radial-flux motors," *IEEE Trans. Ind. Appl*., vol. 48, no. 2, pp. 612-622, Mar./Apr. 2012, doi: 10.1109/TIA.2011.2180495.

[128] S. Niu, S. L. Ho and W. N. Fu, "A novel double-stator double-rotor brushless electrical continuously variable transmission system," *IEEE Trans. Magn.*, vol. 49, no. 7, pp. 3909-3912, Jul. 2013, doi: 10.1109/TMAG.2013.2248347.

[129] L. Mo, L. Quan, X. Zhu, Y. Chen, H. Qiu and K. T. Chau, "Comparison and analysis of flux-switching permanent-magnet double-rotor machine with 4QT used for HEV," *IEEE Trans. Magn*., vol. 50, no. 11, Nov. 2014, Article#: 8205804, doi: 10.1109/TMAG.2014.2331313.

[130] E. Levi, "Multiphase electric machines for variable-speed applications," *IEEE Trans. Ind. Electron*., vol. 55, no. 5, pp. 1893-1909, May 2008, doi: 10.1109/TIE.2008.918488.

[131] I. Zoric, M. Jones and E. Levi, "Arbitrary power sharing among three-phase winding sets of multiphase machines," *IEEE Trans. Ind. Electron*., doi: 10.1109/TIE.2017.2733468.

[132] V. F. M. B. Melo, C. B. Jacobina and N. B. Freitas, "Open-end nine-phase machine conversion systems," *IEEE Trans. Ind. Appl*., vol. 53, no. 3, pp. 2329-2341, May/Jun. 2017, doi: 10.1109/TIA.2017.2669318.

[133] E. Jung, H. Yoo, S.-K. Sul, H.–S. Choi and Y.–Y. Choi, "A nine-phase permanent-magnet motor drive system for an ultrahigh-speed elevator," *IEEE Trans. Ind. Appl*., vol. 48, no. 3, pp. 987-995, May/Jun. 2012, doi: 10.1109/TIA.2012.2190472.

[134] A. Tessarolo, G. Zocco and C. Tonello, "Design and testing of a 45-MW 100-Hz quadruple-star synchronous motor for a liquefied natural gas turbo-compressor drive," *IEEE Trans. Ind. Appl*., vol. 47, no. 3, pp. 1210-1219, May/Jun. 2011, doi: 10.1109/TIA.2011.2126036.

[135] M. Benatmane and T. McCoy, "Development of a 19 MW PWM converter for U.S. Navy surface ships," in *Proc. Int. Conf. Electr. Ship*. Istanbul, Turkey, Sep. 1998, pp. 109-113.

[136] B. Andresen and J. Birk, "A high power density converter system for the Gamesa G10x4,5 MW wind turbine," in *Proc. EPE, Aalborg*, Denmark, 2007.

[137] C. Ditmanson, P. Hein, S. Kolb, J. Mőlck and S. Bernet, "A new modular flux-switching permanent-magnet drive for large wind turbines," *IEEE Ind. Appl.*, vol. 50, no. 6, pp. 3787-3794, Nov./Dec. 2014, doi: 10.1109/TIA.2014.2322135.

[138] J.W. Jansen, M. M. van Lierop, E. A. Lomonova and A. J. A. Vandenput, "Modeling of magnetically levitated planar actuators with moving magnets," *IEEE Trans. Magn*., vol. 43, no. 1, pp. 15-25, Jan. 2007, doi: 10.1109/TMAG.2006.886051.

[139] H.–S. Cho, C.-H. Im and H.-K. Jung, "Magnetic field analysis of 2-D permanent magnet array for planar motor," *IEEE Trans. Magn*., vol. 37, no. 5, pp. 3762-3766, Sep. 2001, doi: 10.1109/20.952708.

[140] M. Kumagai and R. L. Hollis, "Development and control of a three DOF planar induction motor," in *Proc. Int. Conf. Robot. Auto.* (*ICRA*), pp. 3757-3762, May 2012, doi: 10.1109/ICRA.2012.6224612.

[141] P. Dittrich and D. Radeck, "3-DOF planar induction motor," in *Proc. Int. Conf. Electro./Inf. Technol.*, pp. 81-86, May 2006, doi: 10.1109/EIT.2006.252173.

[142] N. Fujii and M. Fujitake, "Two-dimensional drive characteristics by circular-shaped motor," *IEEE Trans. Ind. Appl*., vol. 35, no. 4, pp. 803-809, Jul./Aug. 1999, doi: 10.1109/28.777187.

[143] T. J. Teo, H. Zhu, S.-L. Chen, G. Yang and C. K. Pang, "Principle and modeling of a novel moving coil linear-rotary electromagnetic actuator," *IEEE Trans. Ind. Electron*., vol. 63, no. 11, pp. 6930-6940, Nov. 2016, doi: 10.1109/TIE.2016.2585540.

[144] T. T. Overboom, J. W. Jansen, E. A. Lomonova and F. J. F. Tacken, "Design and optimization of a rotary actuator for a two-Degree-of-Freedom *zphi*-module," *IEEE Trans. Ind. Appl*., vol. 46, no. 6, pp. 2401-2409, Nov./Dec. 2010, doi: 10.1109/TIA.2010.2073430.

[145] J. Si, H. Feng, L. Ai, Y. Hu and W. Cao, "Design and analysis of a 2-DoF split-stator induction motor," *IEEE Trans. Energy Convers*., vol. 30, no. 3, pp. 1200-1208, Sep. 2015, doi: 10.1109/TEC.2015.2418578.

[146] K. J. Meessen, J. J. H. Paulides and E. A. Lomonova, "Analysis of a novel magnetization pattern for 2-DoF rotary-linear actuators," *IEEE Trans. Magn.*, vol. 48, no. 11, pp. 3867-3870, Nov. 2012, doi: 10.1109/TMAG.2012.2199094.

[147] F. C. Williams and E. R. Laithwaite, "A brushless variable-speed induction motor," *Proc. IEE – Part A: Power Eng.*, vol. 102, no. 2, pp. 203-210, Apr. 1955, doi: 10.1049/pi-a.1955.0046.

[148] B. Dehez, G. Galary, D. Grenier and B. Raucent, "Development of a spherical induction motor with two degrees of freedom," *IEEE Trans. Magn.*, vol. 42, no. 8, pp. 2077-2089, Aug. 2006, doi: 10.1109/TMAG.2006.876473.

[149] M. Kumagai and R. L. Hollis, "Development and control of a three DOF spherical induction motor," in *Proc. IEEE Int. Conf. Robot. Auto.* (*ICRA*), pp. 1520-1525, May 2013, doi: 10.1109/ICRA.2013.6630773.
[150] João F. P. Fernandes and P. J. Costa Branco, "The shell-like spherical induction motor for low-speed traction: electromagnetic design, analysis, and experimental tests," *IEEE Trans. Ind. Electron*., vol. 63, no. 7, pp. 4325-4335, Jul. 2016, doi: 10.1109/TIE.2016.2535982.
[151] J. Wang, G. W. Jewell and D. Howe, "Spherical actuators with multiple degrees-of-freedom," in *Proc. IEEE Colloq. Limited Motion Electr. Act. Syst.*, pp. 8/1-8/6, Oct. 1998, doi: 10.1049/ic:19980933.
[152] K. Kahlen, I. Voss, C. Priebe and R. W. D. Doncker, "Torque control of a spherical machine with variable pole pitch," *IEEE Trans. Power Electron.*, vol. 19, no. 6, pp. 1628-1634, Nov. 2004, doi: 10.1109/TPEL.2004.836623.
[153] H. Son and K. M. Lee, "Open-loop controller design and dynamic characteristics of a spherical wheel motor," *IEEE Trans. Ind. Electron*., vol. 57, no. 10, pp. 3475-3482, Oct. 2010, doi: 10.1109/TIE.2009.2039454.
[154] E. Levi, "Advances in converter control and innovative exploitation of additional degrees of freedom for multiphase machines," *IEEE Trans. Ind. Electron.*, vol. 63, no. 1, pp. 433-448, Jan. 2016, doi: 10.1109/TIE.2015.2434999.
[155] K. Matsuse, H. Kawai, Y. Kouno and J. Oikawa, "Characteristics of speed sensorless vector controlled dual induction motor drive connected in parallel fed by a single inverter," *IEEE Trans. Ind. Appl*., vol. 40, no. 1, pp. 153-161, Jan./Feb. 2004, doi: 10.1109/TIA.2003.821805.
[156] M. S. Vicatos and J. A. Tegopoulos, "A doubly-fed induction machine differential drive model for automobiles," *IEEE Trans. Energy Convers*., vol. 18, no. 2, pp. 225-230, Jun. 2003, doi: 10.1109/TEC.2003.811732.
[157] M. Hu, J. Zeng, S. Xu, C. Fu and D. Qin, "Efficiency study of a dual-motor coupling EV powertrain," *IEEE Trans. Veh. Techno*., vol. 64, no. 6, pp. 2252-2260, Jun. 2015, doi: 10.1109/TVT.2014.2347349.
[158] Y. Tang, Dual motor drive and control system for an electric vehicle, US Patent 2010022953 A1, Tesla Motors, Inc., Sep. 2010.
[159] S. Kouro, J. Rodriguez, B. Wu, S. Bernet and M. Perez, "Powering the future of industry: high-power adjustable speed drive topologies," *IEEE Ind. Appl. Magn*., vol. 18, no. 4, pp. 26-39, Jul./Aug. 2012, doi: 10.1109/MIAS.2012.2192231.
[160] S. Tseng, C. Tseng, T. Liu and J. Chen, "Wide-range adjustable speed control method for dual-motor drive systems," *IET Electr. Power Appl*., vol. 9, no. 2, pp. 107-116, Mar. 2015, doi: 10.1049/iet-epa.2013.0291.
[161] E. Ledezma, B. McGrath, A. Munoz and T. A. Lipo, "Dual ac-drive system with a reduced switch count," *IEEE Trans. Ind. Appl*., vol. 37, no. 5, pp. 1325-1333, Sep./Oct. 2001, doi: 10.1109/28.952508.
[162] L. Tang and G. Su, "High-performance control of two three-phase permanent-magnet synchronous machines in an integrated drive for automotive applications," *IEEE Trans. Power Electron*., vol. 23, no. 6, pp. 3047-3055, Nov. 2008, doi: 10.1109/TPEL.2008.2005374.
[163] K. Matsuse, N. Kezuka and K. Oka, "Characteristics of independent two induction motor drives by a four-leg inverter," *IEEE Trans. Ind. Appl*., vol. 47, no. 5, pp. 2125-2134, Sep./Oct. 2011, doi: 10.1109/TIA.2011.2161739.
[164] S. Ito, T. Moroi, Y. Kubo, K. Matsuse and K. Rajashekara, "Independent control of two permanent-magnet synchronous motors fed by a four-leg inverter," *IEEE Trans. Ind. Appl*., vol. 51, no. 1, pp. 753-760, Jan./Feb. 2015, doi: 10.1109/TIA.2014.2332637.
[165] W. Wang, M. Cheng, B. Zhang, Y. Zhu and S. Ding, "A fault-tolerant permanent-magnet traction module for subway applications," *IEEE Trans. Power Electron*., vol. 29, no. 4, pp. 1646-1658, Apr. 2014, doi: 10.1109/TPEL.2013.2266377.